Advances in Science and Technology Research Journal

Advances in Science and Technology Research Journal, 2026, 20(4), 213–226
https://doi.org/10.12913/22998624/214942
ISSN 2299-8624, License CC-BY 4.0

Received: 2025.09.05
Accepted: 2026.02.15
Published: 2026.03.01

Angular dependence of reflected laser radiation intensity during handheld laser welding of structural steel and aluminum alloys

Dawid Stanisz[1], Sławomir Parzych[2], Marek Hebda[2], Małgorzata Cichowlas[3], Joanna Szkudlarek[3], Małgorzata Okrasa[3*]

[1] Prax Weld Sp. z o.o., Łącznik 21A, 33-300 Nowy Sącz, Poland
[2] Faculty of Materials Engineering and Physics, Cracow University of Technology, Warszawska 24, 31-155 Kraków, Poland
[3] CIOP-PIB, Department of Personal Protective Equipment, Wierzbowa 48, 90-133 Łódź, Poland
* Corresponding author's e-mail: maokr@ciop.lodz.pl

ABSTRACT

The growing use of handheld Class 4 laser welding systems raises concerns about operator exposure to reflected and scattered radiation. The purpose of this study is to provide an assessment of the angular distribution and intensity of reflected laser radiation generated during manual welding of structural steel and aluminum alloy in butt and fillet joint configurations. It provides the first angle-resolved and height-resolved experimental characterization of reflected radiation in handheld welding, integrating material reflectivity, joint geometry, and observer position – parameters rarely examined together. Radiation intensity was measured at multiple angles, distances, and heights – including helmet-visor level – under controlled laboratory conditions, using identical welding parameters for both materials. Aluminum, with near-infrared reflectance of ≈75–78% compared with ≈14% for steel, produced broader and more persistent reflection fields. For butt joints, mean maximum intensities were comparable (≈1912 ru for steel and ≈2049 ru for aluminum), but probe orientation and joint type strongly modulated exposure: lateral probe positions yielded ≈2.2-fold higher peak intensities than the forward direction for aluminum and more than fourfold higher for steel, while fillet joints increased the mean maximum intensity for steel by ≈109% relative to butt joints (3997 vs 1912 ru). The most hazardous conditions occurred within 10–15 cm of the weld and at probe angles between 30° and 70°, where both materials generated peak intensities above 1.5×10^4 ru, including at eye level (156 cm), highlighting a substantial risk of ocular overexposure during handheld laser welding. Helmet-level measurements confirmed attenuation of direct radiation. These findings show that effective protection requires PPE with high-optical-density filters, lateral shielding, and an optimized workstation layout, especially when welding reflective materials or working with fillet geometries. Material reflectivity and joint type strongly influence hazard-zone formation, with aluminum and fillet joints presenting the highest risks. Task-specific protective strategies are therefore essential to ensure compliance with exposure limits and maintain operator safety.

Keywords: laser safety, manual laser welding, radiation intensity.

INTRODUCTION

Laser welding systems are gaining increasing importance across diverse industrial sectors owing to their high precision, mobility (in the case of handheld devices), and capability to operate under complex geometric conditions. This technology is widely applied in the automotive and aerospace industries, medical device manufacturing, electronics, and jewelry, enabling the joining of lightweight and difficult-to-weld materials with minimal heat input and high weld quality (1–3). Particularly in sectors requiring flexibility and short production cycles, handheld laser welding allows for efficient fabrication of welds with excellent mechanical properties and a reduced risk

of material distortion (4). Classified as Class 4 lasers according to EN 60825-1 (5), these systems emit high-power radiation that poses a severe hazard to both the eyes and skin. In the context of EN 60825-1, Class 4 designates laser products capable of producing hazardous diffuse and specular reflections, creating potential for immediate injury even at short exposure times. The standard emphasizes the need to implement engineering and administrative controls – including protective housings, beam enclosures, warning systems, controlled access, and mandatory use of appropriate personal protective equipment – whenever operators or bystanders may be exposed to direct or reflected radiation. In manual welding applications, where the beam is used in an open environment and the operator works in close proximity to the interaction zone, these requirements are particularly critical and difficult to fulfil through engineering controls alone. Their operation in open work environments, near the operator, substantially increases the risk of harmful exposure.

Handheld laser welding devices typically employ fiber or Nd:YAG laser sources operating at wavelengths around 1064 nm (near-infrared). These high-power beams emit invisible radiation capable of inducing acute thermal injuries. The eyes are particularly vulnerable, as near-infrared radiation penetrates the cornea and lens, reaching the retina and potentially causing irreversible damage, including retinal burns, cataracts, or photochemical lesions (6–9). In addition to the direct laser beam, welding processes emit broadband optical radiation across ultraviolet (UV), visible, and infrared (IR) ranges, all of which may pose additional risks to operators and nearby workers. A significant hazard also arises from scattered and reflected radiation: during welding, laser beams may reflect unpredictably from workpiece surfaces, generating stray beams that propagate beyond the intended working area (6). Numerous documented incidents show that workers were exposed to hazardous scattered radiation without realizing it. This highlights the need for systematic exposure assessments and well-designed protective measures, particularly in dynamic environments involving mobile, high-power laser systems.

According to European regulations, worker exposure to artificial optical radiation must comply with Directive 2006/25/EC of the European Parliament and of the Council of 5 April 2006, which defines minimum health and safety requirements for exposure to physical agents (artificial optical radiation) (10). This directive obliges employers to assess exposure levels, compare them with exposure limit values, and implement protective measures if limits are exceeded. In the context of laser applications, a key safety parameter is the maximum permissible exposure (MPE), defined as the highest level of irradiance or radiant exposure that can be tolerated by the eyes or skin without causing biological damage. For Class 4 lasers, reliable assessment requires not only the evaluation of direct beam hazards but also the characterization of reflected and scattered radiation levels present in the working environment.

The hazard distance for laser reflections is defined as the distance from the target at which the irradiance of the reflected beam equals the MPE; this distance is termed the reflected nominal ocular hazard distance (R-NOHD) (11). Unlike the standard NOHD, which applies only to the direct laser beam, the R-NOHD accounts for surface reflectivity, the angle and geometry of incidence, and the divergence of the resulting reflected beam. In the case of scattered radiation, exposure assessment is even more challenging, as scattered beams exhibit strong angular dispersion and highly variable intensities that are difficult to measure reliably under real welding conditions.

Given these complexities, research on measuring reflected and scattered laser radiation has intensified in recent years, driven by increasing safety concerns associated with the growing use of high-power lasers in industry. Traditional approaches often relied on laboratory simulations or simplified models, but more advanced methodologies are emerging. For instance, Peckhaus et al. developed a mobile detection system for measuring scattered near-infrared radiation from metallic surfaces, capturing both specular and diffuse components (12). The system, calibrated according to German laser safety standards, was validated under field conditions, demonstrating its effectiveness in identifying hazardous exposure zones (13).

Despite these advances, standardized methodologies for characterizing scattered and reflected radiation in complex and dynamic environments – such as those involving handheld laser welding – remain limited. Current models rarely capture the variability of beam incidence angles, surface conditions, and operator movements inherent in manual welding processes. Furthermore, there is no consensus on sensor placement strategies or on data interpretation protocols that would translate

measurement results into practical exposure assessments for operators and bystanders.

Recent studies in advanced joining and surface engineering have shown that the behavior of metallic surfaces under high-energy processing strongly depends on their microstructure, surface condition, and the presence of oxides or intermetallic phases. This has been demonstrated for aluminum wire bonding (14), laser-assisted surface cleaning used to improve interfacial stability (15), Fe–Al composite coatings (16), and friction-welded S235JR structural steel (17). These findings are relevant for laser safety, as variations in surface roughness, oxidation, thermal history, or phase composition can significantly influence both specular and diffuse reflection components, thereby affecting the propagation of reflected or scattered laser radiation in real industrial environments.

Recent literature has addressed laser back-reflection and safety modelling primarily in the context of automated or fully robotized high-power laser systems, such as industrial laser beam welding, laser-based battery manufacturing, and large-scale high-power research facilities. These studies typically analyze remote or enclosed processes in which the operator is not directly exposed to the laser beam or its reflections. Only a few publications explicitly investigate back-reflected radiation, including analyses of reflections from metallic targets irradiated by high-power laser light (18), simulations of back-reflection amplification in multi-petawatt laser systems (19), and modelling of high-energy laser reflection at sea surfaces for hazard assessment (20). Despite their relevance, none of these studies examine back-reflection behavior or safety modelling in manual (hand-held) laser welding, where the operator remains physically present inside the laser working zone and may be exposed directly to reflected radiation. This absence of data underscores a significant research gap that the present study addresses by analyzing laser beam propagation and reflected radiation specifically under realistic manual welding conditions.

Although the hazard potential of Class 4 handheld laser welding is well recognized, there is a notable lack of experimental data describing how reflected and scattered radiation behave under realistic manual-welding conditions. Existing studies typically rely on stationary optical setups, simplified reflection models, or generic hazard-distance predictions that do not capture the geometric complexity and operator-dependent variability of handheld processes. The novelty of the present work lies in providing one of the first systematic experimental datasets of angular reflection patterns produced during handheld laser welding, offering a level of spatial and angular resolution not previously reported. Additional novelty stems from the direct comparison of two materials with distinctly different reflectivities (structural steel vs. aluminium alloy) and the analysis of two welding joint geometries (butt and fillet), which have not been previously evaluated in a structured way in the context of secondary reflections. Furthermore, the inclusion of angle-resolved measurements, height-dependent observations, and helmet-level exposure assessments enables this study to bridge the gap between theoretical hazard models and practical industrial conditions. Together, these contributions provide an experimental foundation for improving occupational laser safety guidelines in the future.

The purpose of the present study is to perform a detailed analysis of the spatial distribution of reflected and scattered laser radiation generated during manual welding of two commonly used engineering materials: low-alloy structural steel and aluminium alloy. To assess how welding geometry influences exposure, two joint configurations – butt and fillet – were examined systematically. Through this approach, the study aims to identify high-risk exposure zones for observers at various positions, and derive practical recommendations for protective enclosures, workspace layout, and the selection of appropriate personal protective equipment (PPE). In this study, "high-risk exposure zones" refer to areas in which welders or nearby personnel may be exposed to direct or indirect (reflected or scattered) laser radiation at levels that may approach or exceed the applicable MPE. These zones include both the immediate welding area and the surrounding space where hazardous radiation can occur due to reflections from the workpiece or other surfaces.

The remainder of this article is organized as follows: the next section describes the experimental setup, materials, and measurement methodology; this is followed by the presentation of the measurement results and their interpretation; the discussion section examines the implications for occupational exposure and laser safety; and the article concludes with a summary of key findings and directions for future research.

MATERIALS AND METHODS

Measurements of reflected and scattered laser radiation were carried out in a controlled laboratory environment using a handheld fiber laser welding system equipped with a Class 4 high-power single-mode laser source (THEO MA1-65, MaxPhotonics). All experiments were conducted under ambient laboratory conditions with controlled background illumination.

The test specimens consisted of low-alloy structural steel (S235JR) with surface emission coefficient of 0.56 and aluminum alloy (6061) with surface emission coefficient of 0.07, welded in two distinct joint configurations: butt and fillet (Tables 1 and 2, Figure 1). The material samples used in the tests were cut using a laser to final dimensions of 100 × 50 × 5 mm. The S235JR steel samples were prepared from pickled and oiled sheet metal, whereas the aluminum specimens were made from raw 6061 alloy. Prior to the laser emission measurements, all samples were degreased with acetone in accordance with standard preparation procedures to ensure clean and uniform surface conditions.

The laser beam operated at a wavelength of approximately 1080 nm. Welding parameters, including laser power, beam oscillation width, oscillation frequency, and wire feeding speed, were kept constant throughout all trials (Table 3).

The welding parameters listed in Table 3 were selected to reflect values commonly used in industrial practice for the specific joint types, base materials, and material thicknesses investigated. The aim was not to optimize weld quality but to reproduce realistic operating conditions characteristic of handheld laser welding. Using representative process settings ensured that the resulting measurements corresponded to the actual exposure environment within a typical laser welding zone. The inclusion of different joint configurations and material types was intended to simulate the variety of practical scenarios in which welders and nearby personnel may be exposed to reflected or scattered laser radiation.

The reflectance of optical radiation from steel and aluminum samples was determined in accordance with EN ISO 18526-2:2020-09 (21) using a Cary 5E spectrophotometer (Varian, USA) equipped with an Ulbricht integrating sphere. Measurements were performed over the wavelength range of 400–1100 nm.

Laser radiation intensity was recorded with an Ocean Optics HR2000+ spectroradiometer coupled to a VIS-NIR/SR optical fiber (type QP400-2-SR). The measurement system was

Table 1. Basic mechanical properties of structural steel S235JR and aluminum alloy 6061

Strength properties	Low-alloy steel S235JR	Aluminum alloy 6061
Tensile strength (MPa)	360–510	290–320
Yield strength (MPa)	≥ 235	≥ 240
Elongation (%)	≥ 24	8–10

Table 2. Chemical composition of steel S235JR and aluminum alloy 6061

Element, % by mass	Low-alloy steel S235JR	Aluminum alloy 6061
Carbon (C)	max 0.17%	-
Silicon (Si)	max 0.35%	0.4–0.8%
Manganese (Mn)	max 1.40%	max 0.15%
Phosphorus (P)	max 0.035%	max 0.035%
Sulfur (S)	max 0.035%	max 0.035%
Magnesium (Mg)	-	0.8–1.2%
Chromium (Cr)	-	0.04–0.35%
Zinc (Zn)	-	max 0.25%
Titanium (Ti)	-	max 0.15%
Copper (Cu)	-	0.15–0.4%
Iron (Fe)	max 0.7%	-
Aluminum	-	Remainder

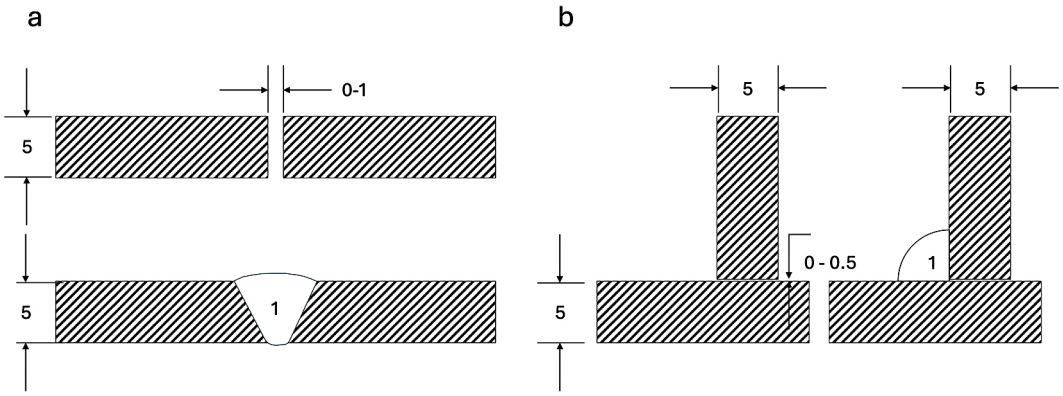

Figure 1. Scheme of the welded specimens and joint configurations: a) butt weld, b) fillet weld

Table 3. Welding parameters depending on the type of material joined

Type of material	Laser beam power [W]	Beam oscillation width [mm]	Beam oscillation frequency [Hz]	Wire feeding speed [mm/s]	Process gas
Low-alloy steel S235JR	1200	2.5	60	8	Nitrogen 5.0
Aluminum alloy 6061	1200	2.5	120	10	Nitrogen 5.0

calibrated using a certified halogen reference lamp OL 200IR (1000 W) powered by a stabilized current source Optronic OL 83A. Based on this calibration, a normalization coefficient of 1.29×10^{-7} can be applied to convert the detector response units (ru) into irradiance-equivalent values (W/m²). This makes full normalization of the recorded spectra possible. However, because the objective of the study was to compare relative differences in radiation intensity between materials, joint types, sensor positions, and observation angles, the results are reported in detector units (ru). Data were collected at different spatial orientations relative to the incident beam, including: (i) in the beam direction from the operator's position, (ii) from a bystander's position at eye level, and (iii) laterally to both sides of the beam at predefined angles (Figure 2).

Measurements were taken at distances (x) from 10–200 cm from the point of laser beam emission. At each distance, recordings were performed at vertical positions (y): (i) the working height corresponding to the welded sample (85 cm), and (ii) average eye levels of a standing operator (135 cm and 156 cm). The selection of the measurement heights was based on anthropometric considerations related to typical working postures in manual laser welding. The height of 85 cm corresponds to the standard working height of industrial welding tables. The height of 135 cm represents the approximate eye level of an operator of average stature (175 cm) leaning forward over the workbench, while 156 cm reflects the eye level of the same operator standing upright. These measurement points therefore correspond to realistic head and eye locations during welding and allow for an accurate assessment of potential laser exposure under practical working conditions (22).

To obtain a comprehensive distribution profile, the detector was positioned at varying angular orientations (α): parallel to the worktable surface (0°) and at incremental tilt angles of 15°, 30°, 45°, 60°, and 75°, enabling the capture of maximal reflection intensities. The selected angles reflect the angular directions in which reflected or scattered radiation may realistically reach personnel under typical manual laser-welding conditions, based on the geometry of the workstation and operator position. Angles above 75° were excluded because radiation at 90° propagates vertically toward the ceiling and therefore does not represent a practical exposure hazard in the working zone. The spectroradiometer sensor was mounted on a tripod to ensure reproducible positioning and alignment.

Additionally, to evaluate direct exposure risks, measurements were repeated with the sensor placed at the visor level of a welding helmet, at a defined distance d from the source. For each angular position and distance, a minimum of five independent readings was recorded. The

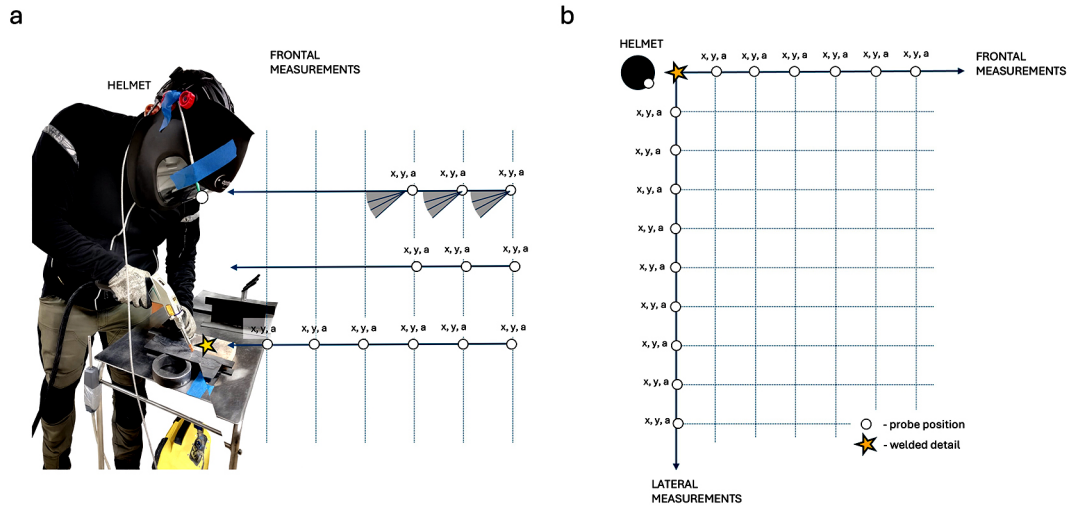

Figure 2. Experimental setup (schematic, not to scale): a) side view, b) bird's-eye view; (x, y, a) = distance from the welding point, sensor height, and sensor angle relative to the horizontal direction.

mean value of these readings was used for further analysis. The variability between repeated measurements remained below 5% for all tested configurations, indicating good repeatability of the measurement procedure. The detection system was calibrated before each measurement series according to the manufacturer's protocol.

RESULTS

Figure 3 presents the spectral reflectance characteristics of the tested materials in the 400–1100 nm range. Aluminum exhibited high reflectance, which decreased gradually toward shorter wavelengths: ≈77.8% at 1100 nm, ≈76–75% between 1064 and 1030 nm, ≈73.4% at 980 nm, ≈65.9% at 808 nm, ≈58.5% at 532 nm, and ≈47.2% at 400 nm. In contrast, steel demonstrated consistently low reflectance values, remaining relatively flat across the spectrum, with a slight increase from ≈13.8% at 1100 nm to ≈14.6% at 400 nm. These results indicate that, in the near-infrared region typical of industrial laser welding (1030–1080 nm), aluminum reflects a substantial proportion of incident radiation, whereas steel reflects only about one-sixth of that amount.

Figure 4 presents the radiation intensity measurements for structural steel (S235JR) and aluminum alloy (6061). The data were acquired for

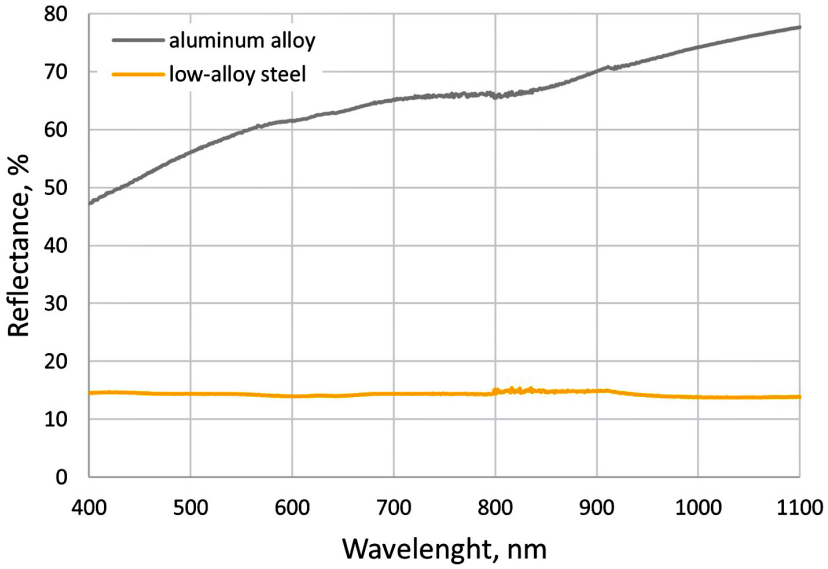

Figure 3. Reflectance of optical radiation for structural steel S235JR and aluminum alloy 6061 samples

butt joint configurations (Figure 1) with the detector positioned in two orientations: (i) forward, aligned with the laser beam axis, and (ii) laterally, offset relative to the beam direction

The results of radiation intensity measurements for fillet joint configurations of low-alloy steel (S235JR) are shown in Figure 5.

Based on the descriptive statistics at 1080 nm, it can be concluded that the maximum recorded radiation intensity during manual laser welding is influenced by multiple factors, including both material properties and measurement geometry. Each factor was analyzed independently, enabling the identification of critical configurations associated with elevated exposure. Nevertheless, under real working conditions these factors may overlap, with secondary reflections further amplifying radiation intensity.

For butt joint configurations, differences between steel and aluminum were relatively small. The mean maximum intensity values were ≈1912 ru for steel and ≈2049 ru for aluminum, indicating comparable exposure levels, with aluminum exhibiting slightly higher averages, most likely due to its higher reflectance (Figure 3).

Probe orientation had a clear and quantifiable influence on the measured radiation intensities. For aluminum, the lateral probe position produced the highest values, with a mean intensity of 2235 ru and a maximum of 15554 ru, compared with a mean of 1921 ru and a maximum of 6959 ru in the forward position. This confirms that lateral scattering from aluminum surfaces generates approximately 2.2 times higher peak intensities than the forward direction. For steel, the effect was even more pronounced. While the forward position yielded a mean intensity of 1329 ru (maximum 10064 ru), the lateral position produced a mean of 5481 ru and a maximum of 15,553 ru–over a fourfold increase in mean intensity relative to the forward direction. These results demonstrate that steel, despite its lower reflectance, can produce extremely strong lateral reflections under certain geometric conditions.

Joint configuration had a strong and quantifiable impact on the measured radiation intensities. For aluminum, only the butt-joint configuration was tested, yielding a mean maximum intensity of 2049 ru and a peak value of 15554 ru. For steel, butt joints produced a mean maximum intensity of 1912 ru (maximum 15109 ru). In contrast, the fillet-joint configuration for steel generated substantially higher values, with a mean maximum intensity of 3997 ru and a peak of 15553 ru. These results demonstrate that fillet joints increased the average maximum intensity for steel by approximately 109% relative to the butt joint (3997 vs. 1912 ru), while producing peak values comparable to the highest intensities observed for aluminum. This indicates that joint geometry is a major determinant of reflection strength, and that fillet joints can create significantly larger hazard zones than butt joints, even for materials with relatively low baseline reflectance such as steel.

Distance from the welding point had a. nonlinear effect on the measured radiation intensities. For aluminum, maximum values occurred at 15 cm, where the mean intensity reached 8685 ru and the peak exceeded 15554 ru, representing the highest aluminum intensities recorded in the study. At shorter (10 cm) and slightly longer (30 cm) distances, mean intensities were markedly lower (1439–1535 ru), and the intensity continued to decline with increasing distance, falling to 1210 ru at 200 cm.

For steel, the highest intensities were also observed at 15 cm, with a mean of 12091 ru and a maximum of 15552 ru, making this configuration the overall peak across all measurements. Elevated mean values persisted up to 30 cm (4101 ru), after which intensity dropped substantially (e.g. 1747 ru at 60 cm, 1565 ru at 90 cm). By 200 cm, the mean intensity decreased to 1091 ru.

These results demonstrate that the most hazardous conditions consistently occur within 10–15 cm of the emission point, where both materials generated maxima above 15500 ru. This localized peak zone represents the primary region of potential overexposure.

Although measurement height is analyzed separately in the manuscript, the combined effect of distance and height confirms that eye-level measurements (156 cm) can capture intensities exceeding 15000 ru, underscoring the occupational relevance of these findings for standing operators positioned near the welding head.

Probe angle had a strong and consistent effect on the measured radiation intensities. For aluminum, the lowest mean intensities occurred at 0° (1090 ru) and 15° (515 ru), while angles between 30° and 70° produced substantially higher values. The mean intensities at 30°, 45°, and 70° were 4695 ru, 1451 ru, and 8847 ru, respectively, with the highest maximum intensity (15554 ru) recorded at 70°.

For steel, the trend was even more pronounced. At small angles (0° and 15°), mean

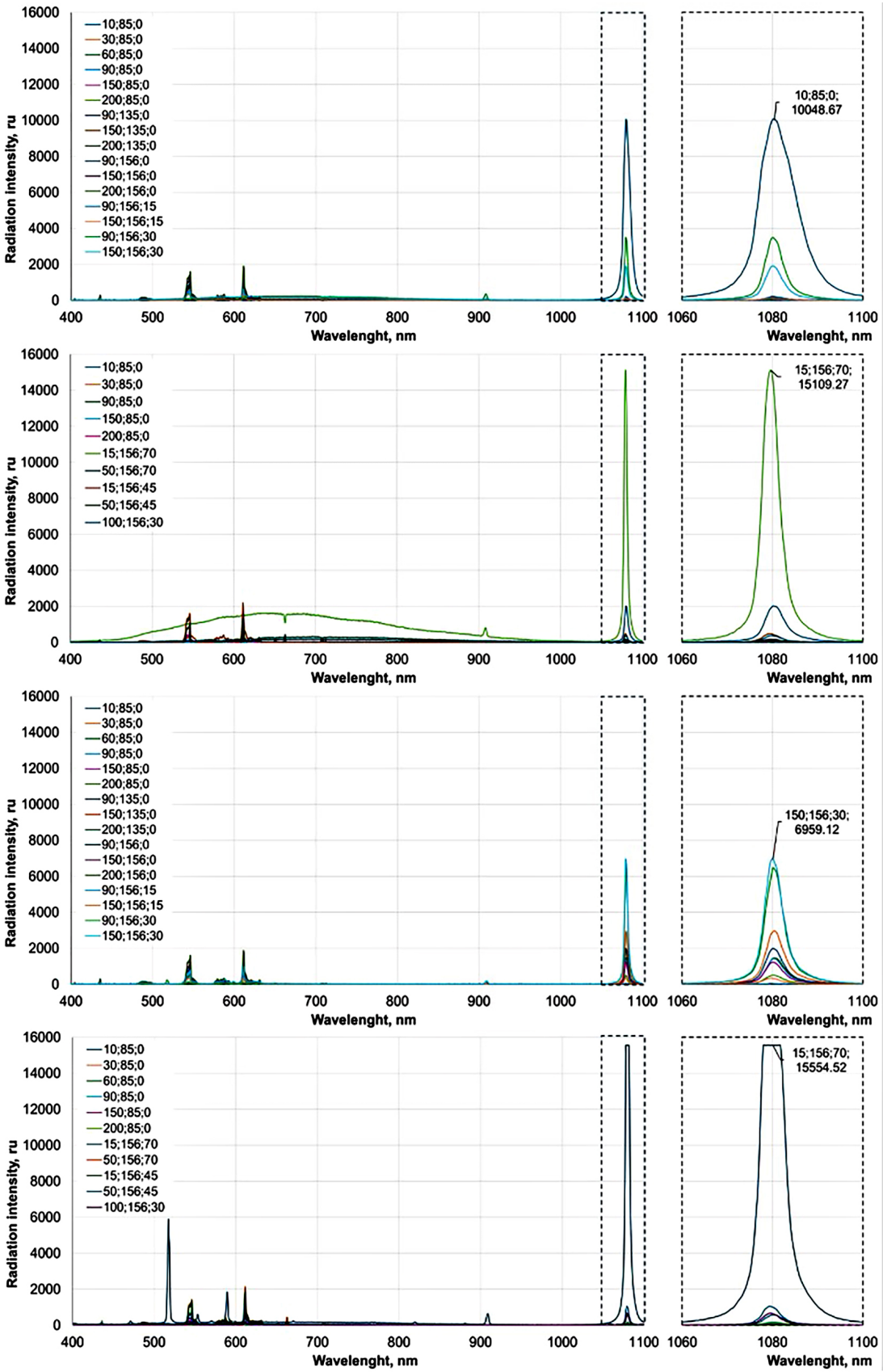

Figure 4. Radiation intensity measurements for butt-welded joints: a) steel sample – forward position, b) steel sample – lateral position, c) aluminum sample – forward position, d) aluminum sample – lateral position; (x, y, a) = distance from the welding point, sensor height, nd sensor angle relative to the horizontal direction. The detailed view of the 1060–1100 nm wavelength range is indicated by a dashed line

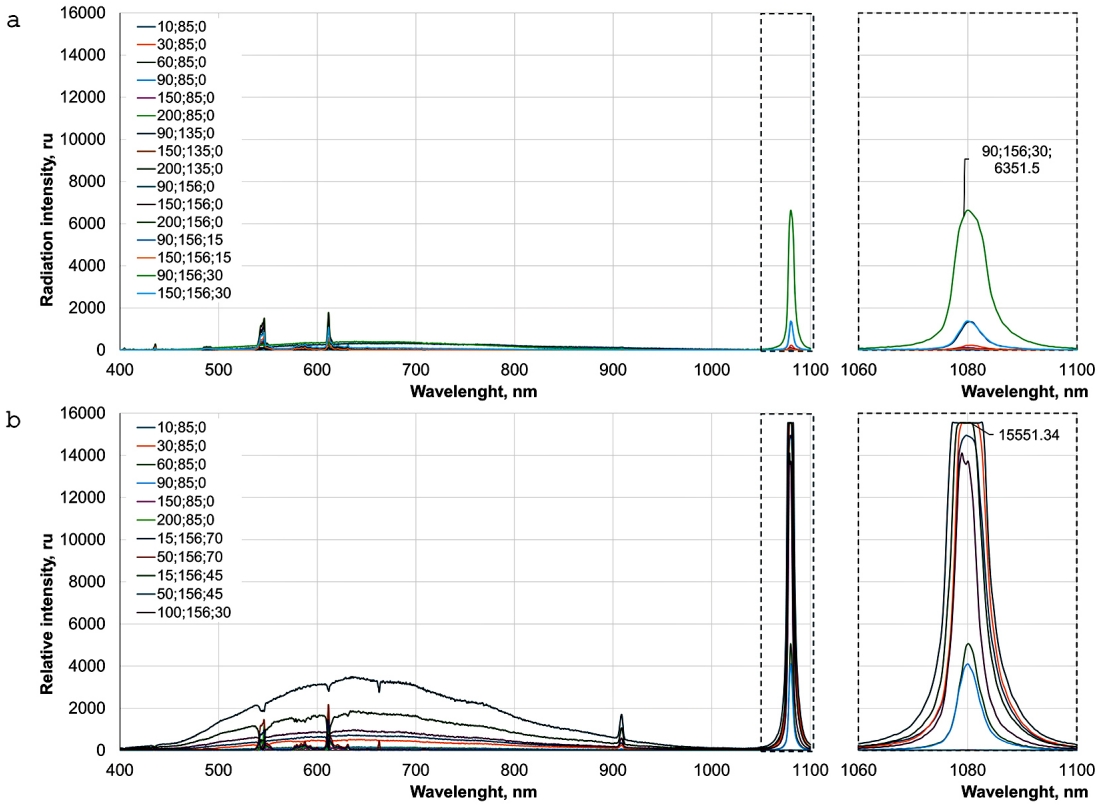

Figure 5. Radiation intensity measurements for fillet -welded joints in steel samples: a) forward position and b) lateral position, shown for different measurement geometries; (x, y, a) = distance from the welding point, sensor height, and sensor angle relative to the horizontal direction. The detailed view of the 1060–1100 nm wavelength range is indicated by a dashed line

intensities were 2058 ru and 561 ru, respectively, but rose sharply at larger angles: 4647 ru at 30°, 5120 ru at 45°, and 8756 ru at 70°. Peak intensities at 30°, 45°, and 70° reached 14090 ru, 15553 ru, and 15551 ru, respectively, consistently forming the highest maxima in the dataset.

These results demonstrate that the greatest exposure risk occurs at sensor angles between 30° and 70°, with 70° yielding the highest average and peak intensities for both materials. Lower angles (0–15°) produced considerably weaker reflections, although isolated high peaks still appeared for steel.

In summary, all investigated factors—material, probe position, joint type, distance, height, and angle – contributed significantly to radiation exposure levels. Several critical configurations were identified in which intensities reached values posing a real hazard to operators' eyesight, reinforcing the necessity of appropriate eye and face protection during handheld laser welding operations.

To approximate realistic operator exposure, additional measurements were performed with the sensor mounted at the visor level of a welding helmet. As shown in Figure 6, these values were consistently lower than the maximum intensities measured near the beam axis; however, they still provide a direct indication of the radiation levels that may reach the eyes during manual welding tasks.

The measurements indicate that a welder positioned behind the laser beam-emitting head is not exposed to direct laser radiation. The helmet-mounted sensor did not detect radiation at the laser emission wavelength (1080 nm), which is consistent with the theoretical principles of light propagation and the laws of physics governing incidence and reflection. However, in the case of more complex joint geometries, multiple reflections of the laser beam may occur, particularly when welding highly reflective materials such as aluminum or copper. Consequently, the possibility of hazardous exposure due to reflected radiation cannot be entirely excluded.

The results demonstrate that manual laser welding can be performed safely, provided that appropriate operational procedures are followed and adequate personal protective equipment

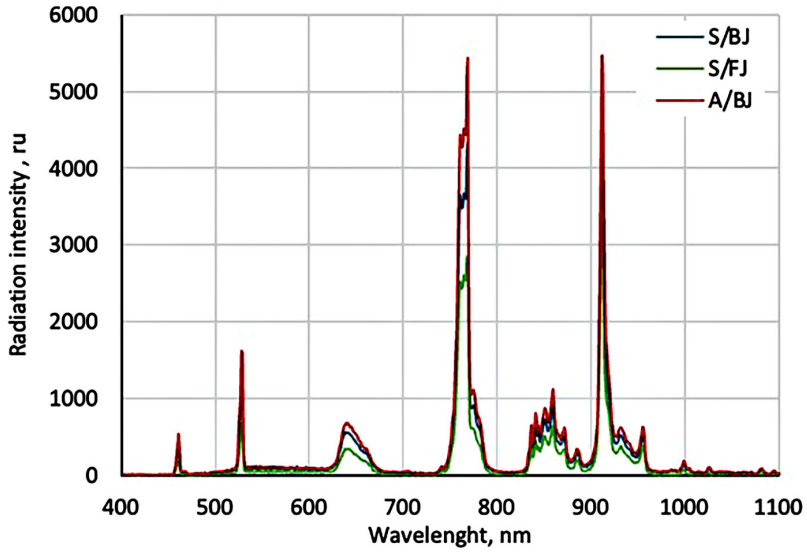

Figure 6. Radiation intensity measurements with the sensor mounted on the welding helmet visor for different configurations: S/BJ – steel and butt joint; S/FJ – steel and fillet joint, and A/BJ – aluminum and butt joint

is employed – specifically, welding helmets equipped with optical filters designed to attenuate radiation at the relevant laser wavelength.

The collected data provide a comprehensive characterization of how radiation intensity depends on material type, joint geometry, sensor placement, and observation angle. These findings form a basis for further evaluation of occupational exposure and the development of evidence-based safety recommendations.

DISCUSSION

The conducted study provides application-oriented insights into the optical hazards associated with manual laser welding. The reflection spectra revealed markedly different reflection behaviors depending on the material. For aluminum, smooth workpiece surfaces combined with a reflectance exceeding 75% at 1030–1064 nm favored strong specular returns; recent studies emphasize that such high reflectivity, particularly before plasma ignition, creates a critical reflection window in which single-bounce reflections may carry sufficient energy to exceed safe levels of radiation (23). Henrichsen et al. showed that reflections from metallic targets can be decomposed into specular, forward-scattered, and Lambertian components, with the specular component producing the largest Nominal Ocular Hazard Distances (NOHD)—up to hundreds of meters under high-power laser conditions (18). While their experiments indicated that most metallic surfaces, including aluminum and steel, tend to reflect predominantly in a diffuse manner, even a small probability of specular reflection can result in disproportionately large hazard distances. This finding highlights that large NOHD values do not necessarily equate to high risk, but that risk assessments must integrate both reflection characteristics and the likelihood of incidental exposure. Retroreflection phenomena, described in recent safety reports (23), further amplify this risk, as beams may be redirected back toward the operator from complex joint geometries. In addition, at visible wavelengths (e.g., 532 nm alignment sources), aluminum maintained appreciable reflectance (~58%), reinforcing the significance of specular reflections. In contrast, steel exhibited substantially lower reflectance (~14%), resulting in weaker but still relevant specular components, particularly under conditions of polished surfaces or grazing incidence. Overall, aluminum presented a considerably higher specular-reflection risk within the near-infrared operating range than steel, with this risk diminishing as the wavelength shifted toward the visible spectrum.

The practical implications of the differing reflective properties of aluminum and steel are particularly important for occupational safety. Aluminum produces strong specular returns that can redirect hazardous energy along narrow angular paths, especially when small changes in the

operator's posture or torch orientation occur. This increases the likelihood that unexpected high-intensity reflections may reach eye level, underscoring the need for robust shielding solutions and PPE with appropriately high optical density during aluminum welding. In contrast, steel's substantially lower reflectance results in weaker scattered radiation which, in several measurement configurations, appeared more dispersed, although the available data do not allow a quantitative determination of the full angular extent. From a practical standpoint, this may require greater attention to workstation layout and lateral shielding to protect assistants and nearby personnel. Overall, these material-dependent behaviors suggest that safety measures for handheld laser welding may benefit from being adjusted to the specific reflective characteristics of the processed material.

Beyond their influence on reflected radiation patterns, the reflective properties of different materials also have important practical implications for welding process efficiency. Highly reflective materials such as aluminum or copper absorb only a limited portion of the incident laser energy, which reduces process stability and restricts the maximum weldable thickness achievable with a given laser power. For instance, using the same laser source, low-alloy steel can typically be welded up to approximately 7 mm, whereas the maximum thickness decreases to around 5 mm for aluminum and to approximately 3 mm for copper due to their progressively higher reflectivity. These process-related constraints further highlight the importance of understanding material reflectivity when assessing both welding performance and occupational safety in manual laser welding applications.

The type of material was found to have a decisive influence on the extent and intensity of scattered and reflected radiation. Low-alloy structural steel (S235JR), which absorbs a large proportion of the laser energy, generated confined hazard zones, with radiation intensity decreasing to near-background levels within 0.8 m of the weld line. By contrast, aluminum alloy 6061, characterized by its high reflectivity, produced far more extensive hazard zones, with measurable radiation persisting at distances beyond 1 m. This highlights a critical and underemphasized risk: welding highly reflective materials such as aluminum or copper necessitates more stringent protective measures than those required for less reflective materials, a distinction insufficiently addressed in existing occupational safety standards.

Joint geometry also exerted a significant influence. Butt joints exhibited relatively simple reflection patterns with well-defined angular maxima, whereas fillet joints generated more complex distributions due to perpendicular surfaces acting as secondary reflectors. This extended the angular range of reflected radiation and increased exposure levels at lateral positions, even at greater distances from the weld. Such geometrically induced secondary reflections are rarely considered in current laser safety models, which typically assume flat or idealized targets (24). While this approach is suitable for generic hazard templates, it does not capture the practical complexity of welding joints with varying geometries. These findings underscore the necessity of considering joint configuration in workplace layout design and emphasize the importance of shielding not only in front of the welding head but also laterally and behind the operator. However, no systematic studies have yet addressed how different joint types (butt, fillet) modify reflection characteristics in handheld laser welding. The present work directly contributes to filling this gap by providing one of the first experimental comparisons of joint-dependent reflection patterns, thereby introducing a novel perspective into laser welding safety research. This highlights the need for targeted investigations to quantify geometry-dependent reflection hazards and to provide an evidence base for refining protective measures.

Helmet-mounted measurements showed that an operator positioned correctly behind the beam source is largely shielded from direct laser radiation. These emissions largely originate from the high-temperature plasma plume above the keyhole, which emits strong UV and blue-light components (9,25). Scattered visible emissions, were measurable during aluminum welding and may affect visual comfort. This justifies the continued use of certified welding helmets equipped with high-optical-density filters (OD $\geq$ 7–9) specifically rated for laser protection, particularly in operations involving reflective materials. In addition, recent optical diagnostics studies show that visible and reflected emissions strongly correlate with process parameters such as laser power, defocus, and keyhole stability (25–27). This dual role of visible radiation—as both a potential hazard and a useful process signal –emphasizes the need for safety filters that block harmful wavelengths while still allowing effective optical monitoring.

Although both steel and aluminum produced comparable peak intensities (~15,000 units) at very short distances (~15 cm), their attenuation profiles differed markedly. Aluminum retained hazardous intensity levels over a greater spatial range, underscoring the need for stricter controls not only for welders but also for assistants and observers in the vicinity. These results provide an empirical basis for defining exclusion zones and enclosure requirements. Barrier heights of at least 2.25 m were determined to be sufficient to protect bystanders from horizontally or upward-scattered radiation, with fire- and laser-resistant enclosure materials recommended to mitigate secondary reflections toward surrounding surfaces or equipment.

Overall, the study validates the necessity of material- and geometry-specific safety considerations in manual laser welding. While international standards such as EN 60825 provide general frameworks, the present findings enable refinement of guidelines related to shielding, PPE, personnel positioning, and training.

CONCLUSIONS

This study provides a experimental assessment of reflected laser radiation during handheld laser welding and shows that both the welded material and joint geometry critically influence hazard-zone formation. Structural steel produced narrow reflection fields with steep attenuation, while highly reflective aluminium generated broader and more persistent angular distributions. Butt joints yielded predictable patterns, whereas fillet joints increased lateral scattering. Measurements at the visor level confirmed that proper operator positioning reduces direct exposure.

In contrast to earlier work focused on stationary setups or simplified reflection models, this study offers one of the first experimental datasets capturing the complexity of handheld Class 4 welding. By integrating material reflectivity, joint geometry, and observation position, the findings demonstrate that handheld welding cannot be evaluated through uniform risk models and that exposure is strongly task-dependent.

The results have direct implications for occupational safety. Protective measures should be tailored to material reflectivity and joint geometry rather than applied generically. Based on reflection intensities, the use of e.g. lateral and rear shielding, protective barriers of at least 2.25 m (compliant with EN 60825-4), and certified welding helmets with high-optical-density filters (EN 207) is recommended. While engineering controls reduce exposure, consistently using properly rated PPE remains the most reliable safeguard. Although economic aspects were not assessed, the findings suggest that appropriate safety measures may support operational efficiency by reducing accidents and downtime.

The study's limitations include the evaluation of two materials, a single wavelength, and controlled laboratory conditions without secondary reflections from surrounding surfaces. These constraints imply that, although the qualitative trends identified here are likely robust, the quantitative values should be verified before broader application—particularly in environments with more complex geometries or variable surface conditions.

The extent to which these findings can be generalized to other materials depends primarily on their optical properties, surface condition, and thermal behavior. The two materials examined in this study—low-reflectivity structural steel and highly reflective aluminum—represent the lower and upper bounds typically encountered in industrial practice. Accordingly, the qualitative trends observed here, such as the widening of hazard zones with increasing reflectivity and the influence of joint geometry on angular scattering, are expected to apply to other engineering metals with comparable characteristics. For materials similar to steel, including stainless steels and titanium alloys, generalization can be made with relatively high confidence. For highly reflective metals such as copper or polished nickel alloys, similar but potentially more intense specular and scattered reflection behavior may occur. However, substantial variation in surface condition—such as oxidation, coatings, roughness, or contamination—can significantly modify reflection patterns and may either amplify or suppress the observed effects. Therefore, material-specific verification is recommended before transferring quantitative values to other systems or workplace configurations.

Future research should examine pulsed lasers, additional industrial wavelengths, and realistic workplace environments where secondary reflections and operator movement alter exposure. Further work on surface conditions—such as oxidation, coatings, and roughness—as well

as on multi-material joints, three-dimensional geometries, and optimized shielding will support improved exposure assessment and updated safety recommendations for handheld laser welding systems.

Acknowledgements

This task was completed based on the results of research carried out within the scope of the 6th stage of the National Programme "Governmental Programme for Improvement of Safety and Working Conditions" funded by the resources of the National Centre for Research and Development. The Central Institute for Labour Protection – National Research Institute is the Programme's main co-ordinator; agreement no. DWP/PNiWP/VI/2023, task no.: I.PN.06.

REFERENCES

1. Markevitch A, Wiener M, Markushov I. Dual-beam lasers meet challenges of the automotive industry: Versatile control of spatial energy deposition lowers the process cost and improves quality and productivity. PhotonicsViews. 2024 ;21(2):52–5. https://doi.org/10.1002/phvs.202400010
2. Cao X, Wallace W, Immarigeon J-P, Poon C. Research and progress in laser welding of wrought aluminum alloys. II. metallurgical microstructures, defects, and mechanical properties. Mater Manuf Process. 2003;18(1):23–49. https://doi.org/10.1081/AMP-120017587
3. Velázquez de la Hoz JL, Cheng K. Investigation on the modeling and simulation of hydrodynamics in asymmetric conduction laser micro-welding of austenitic stainless steel and its process optimization. Proc Inst Mech Eng Part B J Eng Manuf. 2025;239(4):530–43. https://doi.org/10.1177/09544054241235839
4. Moskvitin GV, Polyakov AN, Birger EM. Application of laser welding methods in industrial production. Weld Int. 2013;27(7):572–80. https://doi.org/10.1080/09507116.2012.715953
5. EN 60825-1:2014. Safety of laser products - Part 1: Equipment classification and requirements. Brussels: CENELEC; 2014.
6. Rockwell RJ, Moss CE. Optical Radiation Hazards of Laser Welding Processes Part II: CO_2 Laser. Am Ind Hyg Assoc J. 1989;50(8):419–27. https://doi.org/10.1080/15298668991374912
7. Wolska A, Konieczny P. Promieniowanie laserowe – skutki zdrowotne i aspekty bezpieczeństwa. Prace Instytutu Elektrotechniki. 2006; 228:283–96.
8. Khalimov YS, Vlasenko AN, Tsepkova GA, Sosukin AE. Occupational diseases caused by exposure to laser radiation. Bull Russ Mil Med Acad. 2019;21(2):209–14. https://doi.org/10.17816/brmma25946
9. Schulmeister K, Schmitzer C, Duftschmid K, Liedl G, Schröder K, Brusl H, et al. Hazardous ultraviolet and blue-light emissions of CO_2 laser beam welding. In: International Laser Safety Conference. Laser Institute of America; 1997;229–32. https://doi.org/10.2351/1.5056404
10. Dyrektywa 2006/25/WE Parlamentu Europejskiego i Rady z dnia 5 kwietnia 2006 r. w sprawie minimalnych wymagań w zakresie ochrony zdrowia i bezpieczeństwa dotyczących narażenia pracowników na ryzyko spowodowane czynnikami fizycznymi (sztucznym promieniowaniem optycznym). Dziennik Urzędowy Unii Europejskiej. 2006;L114:38–59. Bruksela: Publications Office of the European Union; 2006.
11. Early E, Megaloudis G. Methodology for Reflected Laser Beam. Hazard Analyses. J Dir Energy. 2010;3:320–42.
12. Peckhaus A, Kuhne P, Neuland M, Hall T, Pargmann C, Duschek F. Development of a radiometric sensor for the hazard assessment of scattered high-power laser radiation. In: Hickman DL, Bürsing H, Kamerman GW, Steinvall O, editors. Electro-Optical and Infrared Systems: Technology and Applications XVIII and Electro-Optical Remote Sensing XV. SPIE; 2021;24. https://doi.org/10.1117/12.2599511
13. Peckhaus A, Elsässer F, Hall T, Duschek F. Field validation of a mobile detection system for laser scattering measurements in the NIR range. In: Hickman DL, Bürsing H, editors. Electro-optical and Infrared Systems: Technology and Applications XIX. SPIE; 2022;10. https://doi.org/10.1117/12.2636087
14. Bieliszczuk K, Zręda J, Chmielewski TM. Selected properties of aluminum ultrasonic wire bonded joints with nickel-plated steel substrate for 18650 cylindrical cells. J Adv Join Process. 2024;9:100197. https://doi.org/10.1016/j.jajp.2024.100197
15. Bieliszczuk K, Zręda J, Chmielewski TM. Influence of cylindrical cells surface cleaning by means of laser ablation on wedge wire bonding process. Coatings. 2024;14:445. https://doi.org/10.3390/coatings14040445
16. Grabias A, Skowro B, Siwek P. Phase structure evolution of the Fe-Al arc-sprayed coating stimulated by annealing. Materials (Basel). 2021;14(3210):1–16. https://doi.org/10.3390/ma14123210
17. Skowrońska B, Chmielewski T, Zasada D. Assessment of Selected Structural Properties of High-Speed Friction Welded Joints Made of Unalloyed Structural Steel. Materials (Basel). 2023;16(93):1–14. https://doi.org/10.3390/ma16010093
18. Henrichsen M, Schwarz G, Ritt G, Azarian A, Eberle

B. Laser safety assessments supported by analyses of reflections from metallic targets irradiated by high-power laser light. Appl Opt. 2021;60(22):F71–87. https://doi.org/10.1364/AO.424722

19. Nistor D, Dumitru AD, Ursescu D, Ticos C, Derycke C, Chalus O. Assessing optical damage risks by simulating the amplification of back-reflection in a multi-petawatt laser system. High Power Laser Sci Eng. 2025;13:1–9. https://doi.org/10.1017/hpl.2025.10049
20. Schwenger F, Azarian A, Henrichsen M. Simulation of the reflection of a high energy laser beam at the sea surface for hazard and risk analyses. Appl Opt. 2024;63(14):3825–41. https://doi.org/10.1364/AO.516715
21. PN-EN ISO 18526-2:2020-09. Ochrona oczu i twarzy - Metody badań - Część 2: Fizyczne właściwości optyczne. Warszawa: PKN; 2020.
22. Tokarski T, et al. Atlas miar człowieka. Warszawa: Centralny Instytut Ochrony Pracy – Państwowy Instytut Badawczy; 2023.
23. American Welding Society. Handheld laser welding safety. AWS Safety & Health Fact Sheet No. 46. Miami (FL): American Welding Society; 2024 Sep.
24. Daigle J-F, Pudo D, Théberge F, Châteauneuf M. Laser safety evaluation for high-energy laser interaction with solids. Opt Eng. 2017;56(2):026106. https://doi.org/10.1117/1.OE.56.2.026106
25. Hietanen M, Honkasalo A, Laitinen H, Lindroos L, Welling I, von Nandelstadh P. Evaluation of hazards in CO_2 laser welding and related processes. Ann Occup Hyg. 1992;36(2). https://doi.org/10.1093/annhyg/36.2.183
26. Horník P, Šebestová H, Novotný J, Mrňa L. Visualization of laser back-reflection distribution during laser welding. IOP Conf Ser Mater Sci Eng. 2021;1135(1):012015. https://doi.org/10.1088/1757-899X/1135/1/012015
27. Gao X, You D, Katayama S. The high frequency characteristics of laser reflection and visible light during solid state disk laser welding. Laser Phys Lett. 2015;12(7):076003. https://doi.org/10.1088/1612-2011/12/7/076003